Comparison of buckling load for H-shaped compression members with different eccentric bracing methods

Y. Kimura[1] & Y. Yoshino[2]
[1]*Tohoku University, Japan*
[2]*Nagasaki University, Japan*

Abstract

In Japanese design code, the bracing for the compression members is supported to be set up on the centroid of its section. On the other hand, the braces may be not jointed at the centroid for the compression members in the real structures, and be eccentrically jointed on the section of members. If non-structural members are used as bracings, it is more effective to design the space frame. These members are supported to be effective to restrain the buckling deformation for the compression members, and then most of non-structural members are plurally or continuously jointed. Our previous papers have evaluated the effect of the eccentric braces to restrain the buckling deformation for H-shaped compression members with an eccentric brace at the center of the member, and with continuously eccentric braces, respectively. But the effect for the continuously eccentric braces may be different from that for an eccentric brace at the center of the compression member. If it makes the effect of each eccentric bracing equivalent, it is more practical to design the compression members with eccentric braces in the space structures.

This paper compares the elasto-plastic buckling behavior for H-shaped compression members with eccentric braces at the center of members to that with continuously eccentric braces, and suggests the unified estimation method for the effect of the bucking restraint for each eccentric bracing.

WIT Transactions on The Built Environment, Vol 120, © 2011 WIT Press
www.witpress.com, ISSN 1743-3509 (on-line)
doi:10.2495/ERES110231

1 Elastic buckling load for H-shaped compression members with different eccentric braces

1.1 Development of elastic buckling load for H-shaped compression members with eccentric different braces

In this section, the elastic buckling load for H-shaped compression members with eccentric braces is developed by the energy method and the eigen-value analyses.

When an H-shaped compression member with eccentric brace is laterally and torsionally buckled, the potential energy U is expressed as the following in reference to Kimura.

Then the flexural and torsional buckling deformation with web distortion occurs as shown in Fig. 1 (Bleich [3]).

$$U = \frac{1}{2}\int_0^l \Big[EI_1 u_1''^2 + EI_2 u_2''^2 + GK_w \beta'^2 + GK_1(\beta' - \alpha_1')^2 + GK_2(\beta' - \alpha_2')^2 + \frac{4D_w}{d}(\alpha_1^2 + \alpha_1\alpha_2 + \alpha_2^2) - P_1 u_1'^2 - P_2 u_2'^2 \Big] dx + \frac{1}{2}\left\{ {}_A K_\beta (\beta - \alpha_1)^2 \Big|_{x=\frac{l}{2}} + {}_A K_u u_0^2 \Big|_{x=\frac{l}{2}} \right\} \tag{1}$$

where EI_i is the flexural rigidity of each flange for H-shaped member, GK_i is the torsional rigidity of each flange and GK_w is the torsional rigidity of web. D_w is the flexural rigidity of web plate for H-shaped members. ${}_AK_u$ is the lateral rigidity of the brace and ${}_AK_\beta$ is the rotational rigidity of the brace. d is the distance between both flanges and l is the length of H-shaped members. P_i and u_i are the compression load and the lateral displacement at the center of the flanges, u_0 is the lateral displacement at the brace point. β is the torsional angle, and α_i is the rotational angles of each flange due to web distortion. The suffix, i, represents 1 and 2, and it means each flange.

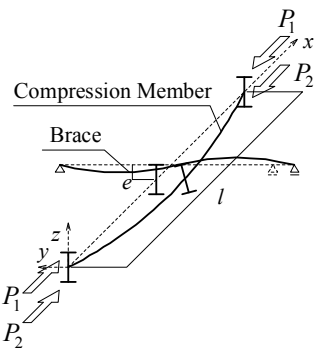

(a) Buckling Deformation for Compression Members

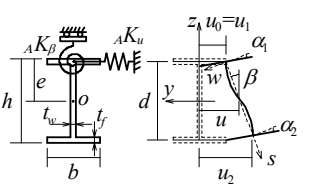

(b) Bracing Models and Buckling Deformation of Section

Figure 1: Buckling deformation for H-shaped compression members with eccentric braces (Type A).

In this paper, it is constantly assumed that the cross section of H-shaped member is symmetric, then $EI_1=EI_2=EI_f$, $GK_1=GK_2=GK_f$ and $P_1=P_2=P_f$. Then it is also assumed that braces are set up at upper flange, so u_0 is equal to u_1.The ratio of eccentric distance to web depth, e/h, is equal to 0.5. Web deformation is expressed in the deflection curve with α_1 and α_2.

$$w = \frac{s(s-d)^2}{d^2}\alpha_1 + \frac{s^2(s-d)}{d^2}\alpha_2 \tag{2}$$

The boundary condition is simple support to strong and weak axis. Lateral deformation of member and web deformation are expressed in the function of sine curves in the following

$$\begin{aligned} u_1 &= a_1 \sin\frac{\pi}{l}x + a_2 \sin\frac{2\pi}{l}x\,, \quad u_2 = b_1 \sin\frac{\pi}{l}x + b_2 \sin\frac{2\pi}{l}x \\ \alpha_1 &= c_1 \sin\frac{\pi}{l}x + c_2 \sin\frac{2\pi}{l}x\,, \quad \alpha_2 = d_1 \sin\frac{\pi}{l}x + d_2 \sin\frac{2\pi}{l}x \end{aligned} \tag{3}$$

Torsional angle, β, is expressed with the lateral deformation of flanges, $u_1$and u_2 as the following

$$\beta = \frac{u_2 - u_1}{d} \tag{4}$$

The lateral deformation, u_1 and u_2 at the center of the member are expressed with the eccentric distance, e and the torsional angle, β_0.

$$u_1 = (e - \frac{d}{2})\beta_0\ ,\ u_2 = (e + \frac{d}{2})\beta_0\ u_1 = (e - \frac{d}{2})\beta_0\ ,\ u_2 = (e + \frac{d}{2})\beta_0 \tag{5}$$

The relationship between the lateral deformation, u_1 and u_2 is obtained from Eqs. (4) and (5) as the following.

$$u_1 = \frac{2e-d}{2e+d}u_2\ u_1 = \frac{2e-d}{2e+d}u_2 \tag{6}$$

In this paper, the eccentric distance e in the range of $e \geq d/2$ is adopted.

Substituting Eq. (6) for Eq. (1), the buckling load P_{cr} is obtained as the following

$$\begin{aligned} P_{cr} = EI_y(\frac{\pi}{l})^2 + \frac{2}{d^2}\{GK_w + (\tau_1+\tau_2)GK_f + \tau_1\frac{2_AK_\beta}{l}(\frac{l}{\pi})^2\} + \frac{2_AK_u}{l}(\frac{l}{\pi})^2 \\ - \sqrt{(\frac{2}{d^2})^2\{GK_w + (\tau_1+\tau_2)GK_f + \tau_1\frac{2_AK_\beta}{l}(\frac{l}{\pi})^2\}^2 + \{\frac{2_AK_u}{l}(\frac{l}{\pi})^2\}^2} \end{aligned} \tag{7}$$

$$P_{cr} = 4EI_y(\frac{\pi}{l})^2 \tag{8}$$

where $P_{cr}=2P_f$ and $EI_y=2EI_f$, τ_1 is the reduction of the rotational rigidity and the upper flange torsional rigidity, and τ_2 is the reduction of the lower flange torsional rigidity. Where l_b is the buckling length. Eq. (7) is the equation for the flexural-torsional buckling load with web deformation. Eq. (8) is the equation for

Euler's buckling load for $l_b=l/2$. Where, the relationship between the torsional angle β_0 and the rotational angle of each flange α_1 and α_2 is expressed with τ_1 and τ_2.

$$\beta_0-\alpha_1=\tau_1\beta_0\ ,\ \beta_0-\alpha_2=\tau_2\beta_0 \tag{9}$$

τ_1 and τ_2 are obtained from Eq. (9) as the following

$$\tau_1=\frac{\frac{6D_w}{d}\{GK_f(\frac{\pi}{l})^2+\frac{2D_w}{d}\}}{\{GK_f(\frac{\pi}{l})^2+\frac{4D_w}{d}+\frac{2\ {}_AK_\beta}{l}\}\{GK_f(\frac{\pi}{l})^2+\frac{4D_w}{d}\}-(\frac{2D_w}{d})^2} \tag{10}$$

$$\tau_2=\frac{\frac{6D_w}{d}\{GK_f(\frac{\pi}{l})^2+\frac{2D_w}{d}+\frac{2K_\beta}{l}\}}{\{GK_f(\frac{\pi}{l})^2+\frac{4D_w}{d}+\frac{2\ {}_AK_\beta}{l}\}\{GK_f(\frac{\pi}{l})^2+\frac{4D_w}{d}\}-(\frac{2D_w}{d})^2} \tag{11}$$

The smaller value of P_{cr} obtained from Eqs. (7) and (8) can be used as the buckling load for H-shaped compression members with eccentric braces. Similarly, elastic buckling load for H-shaped compression members with continuously eccentric braces is obtained by the energy method and the eigen-value analyses. When H-shaped compression member with continuously eccentric brace is laterally and torsionally buckled, the potential energy U is expressed as the following in reference to Kimura and Amamoto [2].

Then the flexural and torsional buckling deformation with the web distortion occurs as shown in Fig. 2 (Bleich [3]).

$$U=\frac{1}{2}\int_0^l\Big[EI_1u_1''^2+EI_2u_2''^2+GK_w\beta'^2+GK_1(\beta'-\alpha_1')^2+GK_2(\beta'-\alpha_2')^2 \\ +\frac{4D_w}{d}(\alpha_1^{\ 2}+\alpha_1\alpha_2+\alpha_2^{\ 2})-P_1u_1'^2-P_2u_2'^2\Big]dx+\frac{1}{2}\Big\{{}_BK_\beta(\beta-\alpha_1)^2+{}_BK_uu_0^{\ 2}\Big\} \tag{12}$$

$${}_AK_u={}_BK_u l\ ,\ {}_AK_\beta={}_BK_\beta l \tag{13}$$

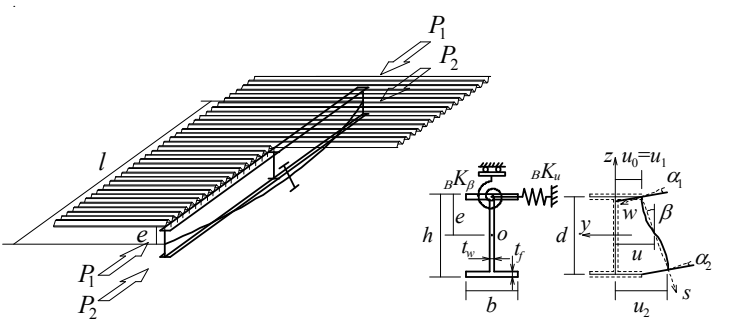

(a) Buckling Deformation for Compression Members

(b) Bracing Models and Buckling Deformation of Section

Figure 2: Buckling deformation for H-shaped compression members with continuously eccentric braces (Type B).

Then it is defined that the case of the rigidity multiplied by length of members in eq. (13) is equivalent to the bracing rigidity for the case of eccentric braces at the center of members as Eqs. Lateral deformation of member and web deformation are expressed in the function of sine curves in the following

$$u_0 = u_1 = a_1 \sin\frac{n\pi}{l}x\,, \quad u_2 = a_2 \sin\frac{n\pi}{l}x$$
$$\alpha_1 = b_1 \sin\frac{n\pi}{l}x\,, \quad \alpha_2 = b_2 \sin\frac{n\pi}{l}x \tag{14}$$

Substituting Eq. (6), (14) for Eq. (12), the buckling load P_{cr} is obtained as the following

$$P_{cr} = EI_y(\frac{n\pi}{l})^2 + \frac{2}{d^2}\{GK_w + (\tau_1+\tau_2)GK_f + \tau_1 {}_BK_\beta(\frac{l}{n\pi})^2\} + {}_BK_u(\frac{l}{n\pi})^2$$
$$-\sqrt{(\frac{2}{d^2})^2\{GK_w + (\tau_1+\tau_2)GK_f + \tau_1 {}_BK_\beta(\frac{l}{n\pi})^2\}^2 + \{{}_BK_u(\frac{l}{n\pi})^2\}^2} \tag{15}$$

The buckling load for H-shaped compression members with continuously eccentric braces is obtained from Eq. (15), with the order of buckling mode, n, for the lowest buckling load in this equation. Eq. (15) is the equation for the flexural-torsional buckling load with web deformation. τ_1 and τ_2 is obtained from Eq. (9) as the following

$$\tau_1 = \frac{\frac{6D_w}{d}\{GK_f(\frac{n\pi}{l})^2 + \frac{2D_w}{d}\}}{\{GK_f(\frac{n\pi}{l})^2 + \frac{4D_w}{d} + {}_BK_\beta\}\{GK_f(\frac{n\pi}{l})^2 + \frac{4D_w}{d}\} - (\frac{2D_w}{d})^2} \tag{16}$$

$$\tau_2 = \frac{\frac{6D_w}{d}\{GK_f(\frac{n\pi}{l})^2 + \frac{2D_w}{d} + {}_BK_\beta\}}{\{GK_f(\frac{n\pi}{l})^2 + \frac{4D_w}{d} + {}_BK_\beta\}\{GK_f(\frac{n\pi}{l})^2 + \frac{4D_w}{d}\} - (\frac{2D_w}{d})^2} \tag{17}$$

Fig. 3 shows the numerical analysis model for the H-shaped compression members with eccentric brace. Marc 2008 is used for the numerical analyses. Type A represents the eccentrically braced members at the center of structural members, and Type B represents structural members with continuously eccentric braces. The compression member consists of 4 node shell elements, and the eccentric brace is replaced on the lateral and rotational springs. In Type B, The spacing between bracings, l', is equal to 250 mm. Then the value of lateral and rotational rigidity of springs are calculated as ${}_BK_u l'$ and ${}_BK_\beta l'$, respectively. The boundary condition is simple supports to strong and weak axis, and three kinds of the cross-sectional shapes are adopted as shown in Table 1.

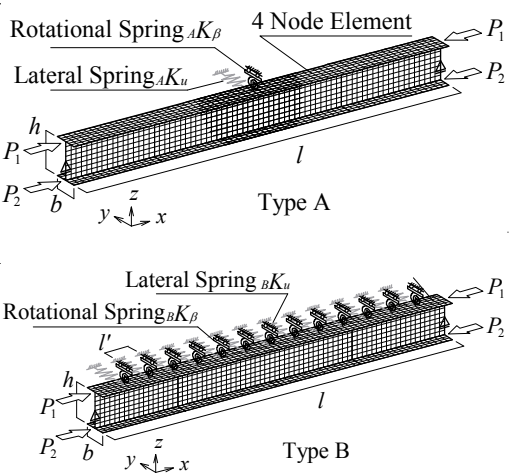

Figure 3: Numerical analysis models.

Table 1: Cross-sectional shape of H-shaped members.

b/h	h	b	t_w	t_f	
0.5	300	150	6.5	9	
0.68	294	200	8	12	
1	300	300	10	15	(mm)

1.2 Comparison of equivalent bracing rigidity for H-shaped compression members with different eccentric braces

Fig. 4 shows the relationship between the elastic buckling stress, σ_{cr}, for H-shaped compression members with eccentric braces and slenderness ratio, λ.

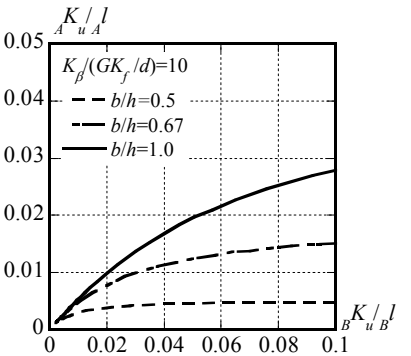

Figure 4: Elastic buckling stress for H-shaped compression members with eccentric braces.

The buckling load for H-shaped compression members with eccentric braces (in Type A) is obtained from Eqs. (8) and (9), and the smaller value of P_{cr} obtained from both expressions, is used. The buckling load for the case of continuously eccentric braces (in Type B) is obtained from Eq. (16). For the small slenderness ratio, if bracing rigidity in Type A is equal to that in Type B, ${}_AK_u={}_BK_ul$, ${}_AK_\beta={}_BK_\beta l$, the elastic buckling stress in Type A is constantly higher than that in Type B. In this case, the buckling stress for Type A is equal that for Type B, when the lateral and rotational rigidity of Type A (K_u,K_β) is in half of that for Type B (${}_BK_u$=0.5 ${}_AK_u$, ${}_BK_\beta$=0.5 ${}_AK_\beta$), respectively. In addition, the buckling stress for Type B with n=2 is constantly higher than that for perfect support for Type A. Then the plots ▼, ▽ in Fig. 4 are the points to change from the lateral-torsional buckling to Euler's Buckling for $l_b=l/2$ in Type A, and ▼ in Fig.4 is the point to change from the buckling load for n=1 to buckling load for n=2 in Type B.

Fig. 5 shows the relationship between the lateral rigidity ratio, ${}_AK_u/{}_Al$ for Type A and that, ${}_BK_u/{}_Bl$ for Type B, when the bucking mode changes such as the plots, ▼, ▽ and ▼ in Fig. 4.

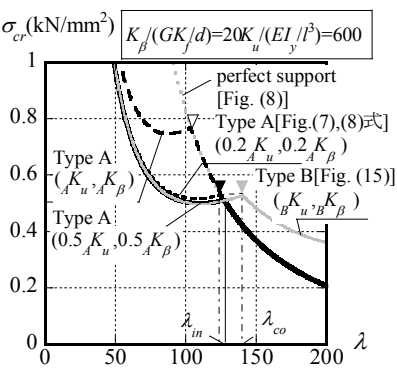

Figure 5: Comparison of lateral rigidities between Type A and Type B.

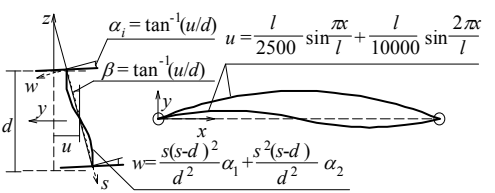

Figure 6: Initial impressions.

${}_AK_u/{}_Al$, and ${}_BK_u/{}_Bl$ are expressed as the ratio of the lateral rigidity to length for Type A and for Type B. The parameter is the cross-sectional shape. The lateral rigidity ratio for Type B, ${}_BK_u/{}_Bl$, is constantly higher than that for Type A, ${}_AK_u/{}_Al$. It is shown that wide flange, b/h=1.0, requires the higher rigidity, ${}_AK_u/{}_Al$ than the other at the some ${}_BK_u/{}_Bl$.

2 Evaluation of elasto-plastic buckling stress for H-shaped compression members with different eccentric bracings

2.1 Elasto-plastic buckling behavior for H-shaped compression members with different eccentric bracings

In this section, elasto-plastic buckling behavior for H-shaped compression members with eccentric braces at the center of the members and with continuously eccentric braces is confirmed by the elasto-plastic large deformation analyses. Marc version 2008 is used [MSC, 2008]. The analyses models and boundary condition are same as the eigen-value analyses models in the previous section. Material properties for H-shaped members are shown in Table 2. Initial impressions of the lateral displacement, u, the torsional angle, β, and the rotational angle of each flange due to the web distortions, α_i, are described as the function of sine curves in the followings.

$$u = \frac{l}{2500}\sin\frac{\pi x}{l} + \frac{l}{10000}\sin\frac{2\pi x}{l} \tag{18}$$

$$\beta = \tan^{-1}(u/d) \tag{19}$$

$$\alpha_i = \tan^{-1}(u/d) \tag{20}$$

where the suffix i represents 1 and 2, and it means each flange. The web distortion is expressed in the deflection curve with α_1 and α_2 as the following.

Table 2: Material properties of H-shaped members.

E (kN/mm^2)	E_{st} (kN/mm^2)	σ_y (N/mm^2)	σ_u (N/mm^2)
206	2.74	294	436

In this section, the lateral and rotational rigidities of braces are expressed as the ratio of rigidities of braces to minimum required rigidities, K_u/K_{u0} and $K_\beta/K_{\beta 0}$. For continuously eccentric bracing, the value of the bracing rigidity from n=1 to n=2 is defined as the required rigidity. The coordinates K_u/K_{u0} and $K_\beta/K_{\beta 0}$ at the required rigidity are expressed as k_0. For numerical analyses, four points on the curve of k_0 in Fig. 7 are selected, and these coordinates are expressed as K_M, $2.5K_B$, $5K_U$ and $10K_U$. When a distance from (K_u/K_{u0}, $K_\beta/K_{\beta 0}$)=(1,1) to the curve of k_0 is shortest, the coordinates K_u/K_{u0} and $K_\beta/K_{\beta 0}$ on the curve of k_0 are defined as K_M. For $2.5K_B$ the value of $K_\beta/K_{\beta 0}$ on the curve of k_0 is fixed at 2.5, and then the value of K_u/K_{u0} depends on cross-sectional shapes and slenderness ratio. For $5K_U$ and $10K_U$, the value of K_u/K_{u0} on the curve of k_0 is fixed at 5.0 and 10, and then the value of $K_\beta/K_{\beta 0}$ depends on cross-sectional shapes and slenderness ratio. Non-structural members in the real truss structures have less than the required rigidity, so that $0.25k_0$ to $0.5k_0$ of bracing rigidities are selected as the analytical parameters in Appendix. For example, the coordinates on the curve of $0.5k_0$ are half of the coordinate on the curve of k_0, thus the values of K_u/K_{u0} and $K_\beta/K_{\beta 0}$ for $0.5k_0$ are half of these for k_0, respectively.

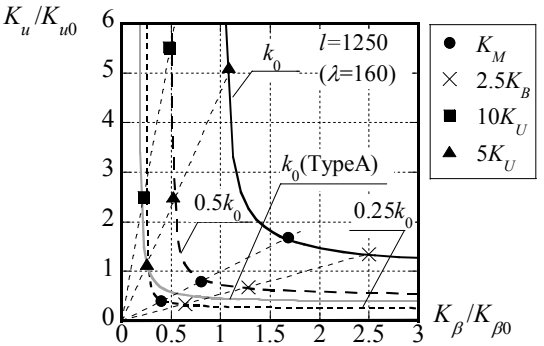

Figure 7: Lateral and rotational rigidity of continuously eccentric braces.

Fig. 8 shows the elasto-plastic buckling behavior for H-shaped compression members with different type of braces. Figs. 8 (a)~(d) represent the relationship between the compression load, P/P_y, the lateral displacement, u/l, the torsional angle, β, the rotational angle of each flange due to the web distortions, α_1, α_2, and the axial displacement, δ/δ_y, respectively. Then the plots ▼, ▼ in Fig. 8 (a) are the points at the maximum load, P_m, and ▽, ▽ in Fig. 8 (a) are the yielding points. Where the maximum load, P_m, is defined as the elasto-plastic buckling load. u, β, α_1 and α_2 in Figs. 8 (b)~(d) are the displacement at the center of members. The elasto-plastic buckling load, P_m, for Type A with $2.5K_B$ is almost equal to that for Type B. On the other hand, the elasto-plastic buckling load, P_m, for Type B with $10K_U$ is much larger than that for Type A with $10K_U$. The torsional angle, β , at P_m for Type B with $10K_U$ is larger than that for Type A.

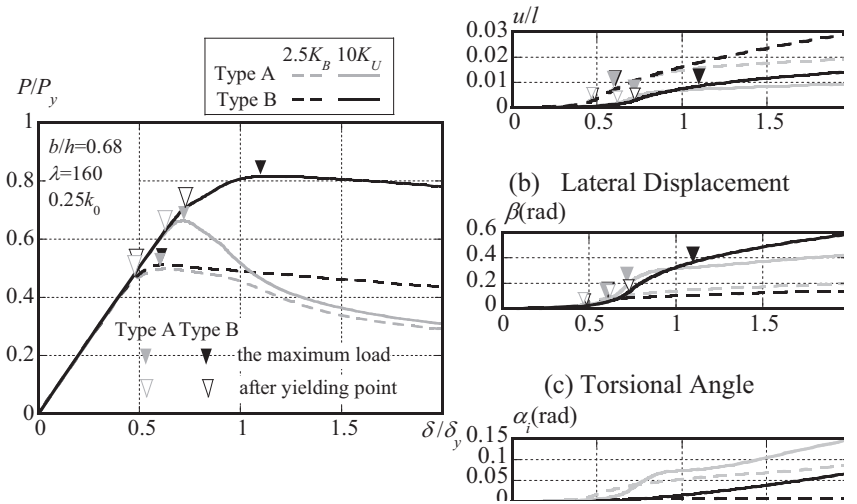

Figure 8: Elasto-plastic buckling behavior for H-shaped compression members with eccentric braces.

After yielding, the torsional angle, β, for Type B increase rapidly. After yielding for H-shaped compression members, the reduction in the torsional rigidity for members is small, even though the torsional angle is larger. Then the members keep their strength after the members are inelastically buckled.

Fig. 9 shows the relationship between the lateral displacement, u_1, and the torsional displacement, u_2-u_1, at P_m for different type of bracing rigidity.

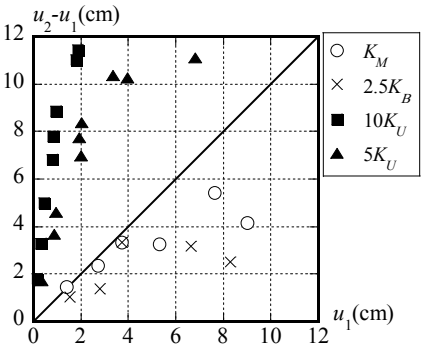

Figure 9: Relationship between lateral displacement and torsional displacement.

u_1 is the lateral displacement of upper flange, and u_2-u_1 is the difference of lateral deformation between upper and lower flanges at P_m . Then for fig. 9, u_1 and u_2-u_1 is defined as lateral displacement and torsional displacement. For K_M and $2.5K_B$, the lateral displacement, u_1, is much larger than the torsional displacement,u_2-u_1, and for $10K_U$ and $5K_U$, u_2-u_1 is much larger than u_1. When the lateral displacement is larger than the torsional displacement, the buckling mode of H-shaped members is called as the predominantly lateral buckling mode. Similarly, when the torsional displacement is larger than the lateral displacement, the buckling mode of H-shaped members is called as the predominantly lateral buckling mode. Therefore, the buckling mode for K_M, $2.5K_B$ is predominantly lateral buckling mode and The buckling mode for $10K_U$, $5K_U$ is predominantly torsional buckling mode. The relationship between the predominantly bucking deformation and the buckling stress must be investigated.

2.2 Elasto-plastic buckling behavior for H-shaped compression members with different eccentric bracings

Fig. 10 show the relationship P_m for Type A and that for Type B. Fig. 10(a) compares the buckling load for the for Type A with or without the vertical stiffener, and Fig. 10(b) show the buckling load for the different type of braces. For Type A, the elasto-plastic buckling load, P_m, with the vertical stiffener is larger than that without the vertical stiffener, because the web distortion is restrained by the vertical stiffener. For predominantly lateral buckling mode, the elasto-plastic buckling load, P_m for Type A is almost equal to that for Type B.

On the other hand, for predominantly lateral buckling mode, the elasto-plastic buckling load, P_m for Type B with $10K_U$ and $5K_U$ is higher than that for Type A, because the torsional rigidity for Type A is higher than that of Type B due to continuously eccentric bracing.

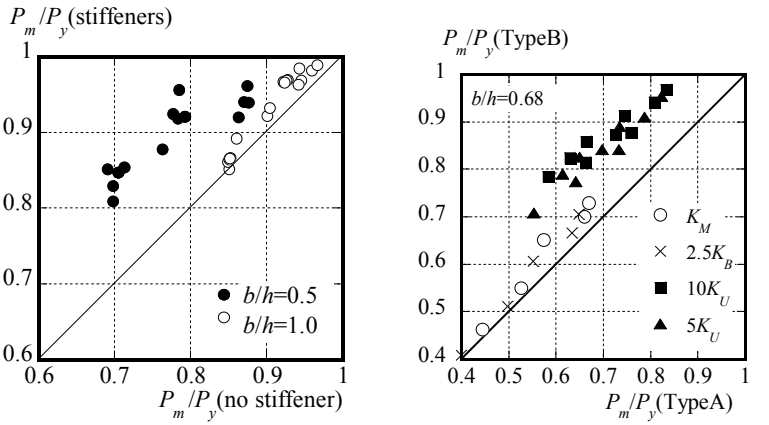

(a) with or without the vertical stiffener (b) different type of braces

Figure 10: Relationship elasto-plastic buckling load.

Fig. 11 shows the relationship between lateral rigidity ratio ${}_BK_u/{}_BK_{u0}$, and the modified ratio, ${}_B\bar{K}_u/{}_BK_{u0}$ for Type B. The plots represent the numerical analyses results for three kinds of the cross section. H-shaped members for Type B possess the only elasto-plastic buckling load for Type A with ${}_B\bar{K}_u/{}_BK_{u0}=1({}_AK_u/{}_AK_{u0}=1)$, even though ${}_BK_u/{}_BK_{u0}$ for Type B increases. The curve closed from solution of Eq. (21) is represented as the following in reference to the numerical analyses results.

$$ {}_B\bar{K}_u/{}_BK_{u0} = 1-0.3\sqrt{{}_BK_{u0}/{}_BK_u} \tag{21} $$

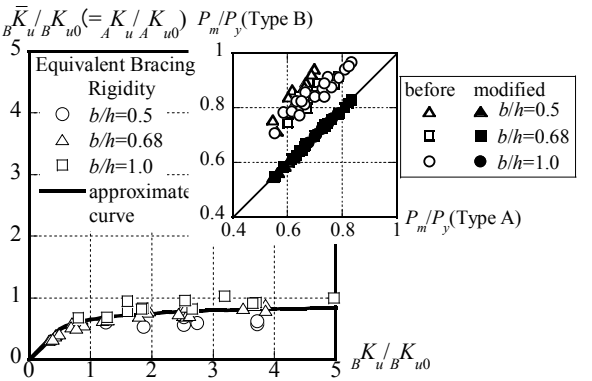

Figure 11: Evaluation of equivalent bracing rigidity.

Then the elasto-plastic buckling load for Type A and Type B can be evaluated using the equivalent rigidity of eq. (21).

3 Conclusion

1) When the buckling mode of H-shaped members is the predominantly torsional buckling mode, the elasto-plastic buckling load for Type B is higher than that for Type A.
2) When the buckling mode is the predominantly torsional buckling mode, the equivalent bracing rigidity for the elasto-plastic buckling load of type A equal to that for Type B is obtained from Eq. (21).
3) When the buckling mode is the predominantly torsional buckling mode, the equivalent bracing rigidity for the elasto-plastic buckling load of type A equal to that for Type B is obtained from Eq. (21).

Appendix

Fig. A1 shows the coordinates of bracing rigidity of non-structural members for the real truss structure. Symbols show the case of non-structural members with channel section and angle section. The black solid curve represents the case of required bracing rigidity. According to Fig. A1, part of the non-structural member does not possess the required bracing rigidity.

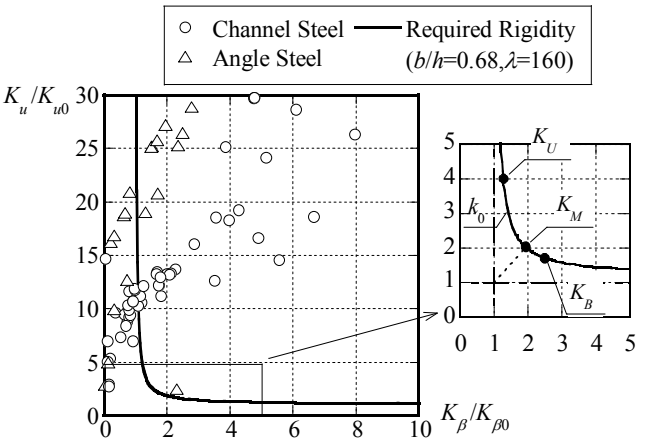

Figure A1: Bracing rigidity of non-structural members for real truss structures.

References

[1] Y Kimura, A Amamoto (2006). Effect of Web Deformation on Buckling Load for H-Shaped Compression Member with Eccentric Braces, Journal of Structural Construction Engineering, AIJ. 600, 187-194 (in Japanese)

[2] Y Kimura, A Amamoto (2009). Effect of Lateral and Rotational Restraint for Eccentric Braces on Flexural-Torsional Buckling Load with Web Deformation for H-Shaped Compression Members AIJ. 637, 583-591 (in Japanese)
[3] Hans H Bleich (1952). Buckling Strength of Metal Structures, McGraw-Hill Book Co., 142-147.